

CHAPTER 4 NUMERICAL METHOD

It should be recalled that for the threshold channel case (for which no sediment motion takes place), specifying either water discharge Q , or channel slope S , is sufficient to produce a unique solution for the flow system. For the case of an optimal stable channel, however, the addition of sediment discharge Q_s , provides an additional degree of freedom. Thus, in order to obtain a unique solution, one must specify either Q and S , Q and Q_s , or S and Q_s . The numerical scheme can easily be modified to accommodate several possible design scenarios. Four commonly encountered situations and their corresponding solution procedures are considered here.

4.1. SLOPE AS AN INDEPENDENT VARIABLE

In the following two schemes, water discharge Q and channel slope S are assumed to be given, and sediment discharge Q_s is assumed to be a dependent variable. The first scheme applies to channels with a dimensionless flat-bed width B_f^* that is less than or equal to 5.0. These shall be referred to as ‘narrow’ channels. The second scheme is used for channels with B_f^* greater than 5.0; from hereon referred to as ‘wide’ channels. The differences between narrow and wide channels, which necessitate that they be considered separately, will be covered in the next chapter. The two schemes are illustrated by the flowchart of Figure 4.1.

4.1.1. NARROW CHANNEL

Given: grain sizes d_{50} and d_{90} , water discharge Q , dimensionless critical shear stress τ_{cr}^* , and longitudinal channel slope S .

Find: center depth D_c , dimensionless critical stress-depth δ_{cr}^* , bank width B_s^* , flat-bed width B_f^* , bank shape, and sediment transport rate for flat-bed region Q_s .

1) The parameters μ and β are specified. A value for the dimensionless critical bed-stress depth δ_{cr}^* is assumed. The value of D_c is calculated using the equation for the Shields stress:

$$D_c = \frac{R_s \tau_{cr}^* d_{50}}{S \delta_{cr}^*} \quad (20)$$

2) The value of d^2D^*/dy^{*2} at the junction point is assumed. From experience, reasonable values would be between -1.9 and -2.0. Knowing that $D^* = 1$ and $dD^*/dy^* = 0$ at the junction point, the value of d^3D^*/dy^{*3} is calculated using Equation 4.

3) Starting with these data at the junction point, the values of D^* , dD^*/dy^* , d^2D^*/dy^{*2} , d^3D^*/dy^{*3} at the next grid point along the bank are determined using a Runge-Kutta-Merson scheme, which is of $(\Delta y^*)^5$ order (de Vahl Davis, 1986), Δy^* being the step-size. The advantage of this numerical scheme is that it gives an idea of the local truncation error associated with a given step-size. This allows the step-size to be adjusted so that the error is kept within acceptable limits, and at the same time, makes sure a step-size is not smaller than necessary. The values of D^* , dD^*/dy^* , d^2D^*/dy^{*2} , and d^3D^*/dy^{*3} at succeeding grid points are determined in a similar manner.

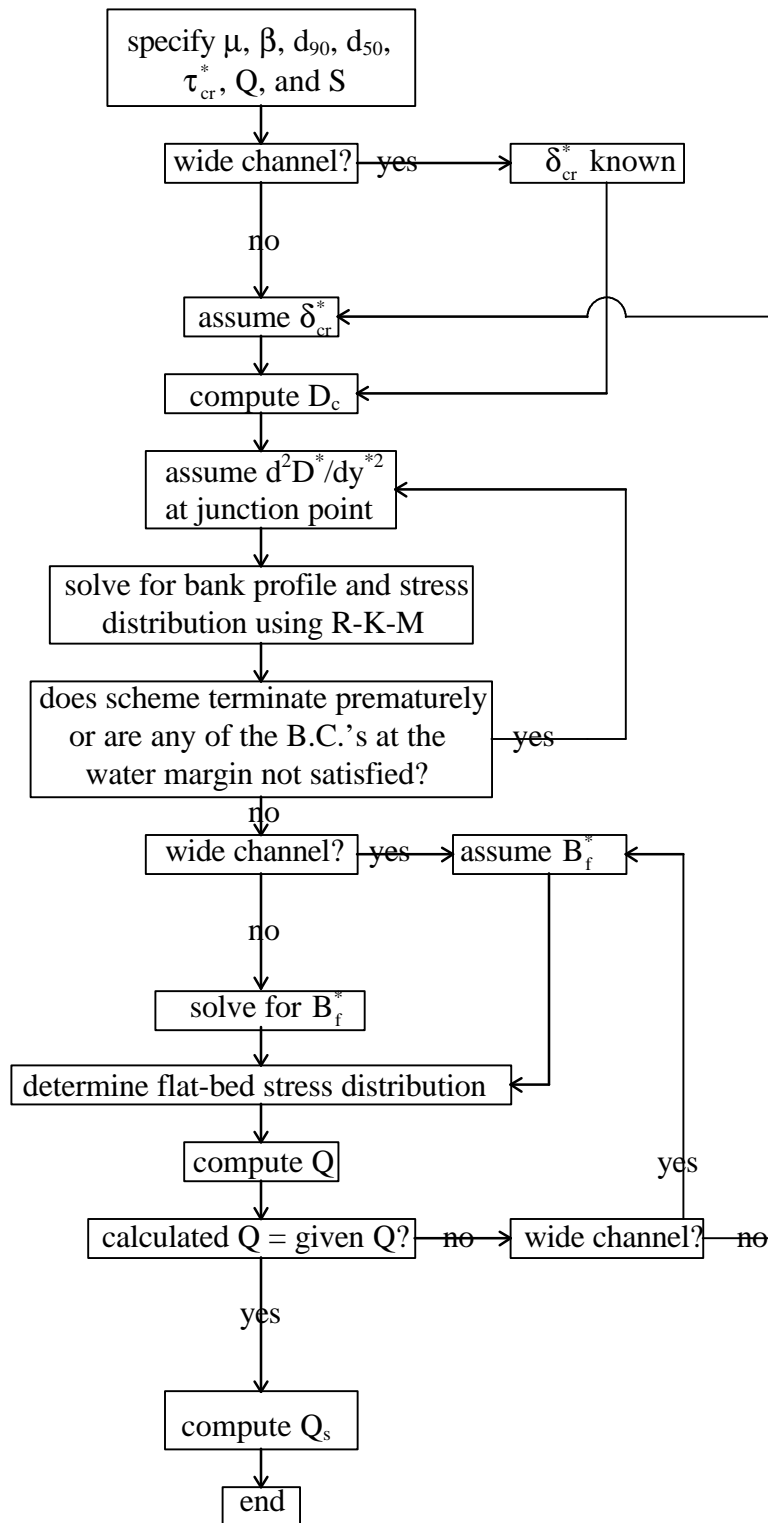


Figure 4.1. Flowchart for the case of Q_s being the dependent variable

If the scheme terminates prematurely, or if upon reaching the water margin the boundary conditions $D^* = 0$ and $dD^*/dy^* = -\mu$ are not satisfied, the value for d^2D^*/dy^{*2} is updated using the half-interval method (de Vahl Davis, 1986). Steps 2 and 3 are repeated until the water margin is reached and both boundary conditions there are satisfied. At this point, the shape of the bank region will have been determined. Since this represents a threshold bank profile, the fluid shear stress coincides with the critical stress at every point along the bank. The stress-depth distribution is thus determined using Equation 3 (the force-balance equation). Aside from determining the value of stress-depth δ_{crb}^* at each grid point along the bank, the values of $d\delta_{crb}^*/dy^*$ and $d^2\delta_{crb}^*/dy^{*2}$ are calculated using equations derived by differentiating Equation 3 twice with respect to y^* . At this point the bank solution is complete.

4) A value for $d\delta^*/dy^*$ at the junction point will have been obtained from the bank solution. Plugging this into Equation 11, which ensures that lateral momentum flux at the junction point is continuous, gives the value for $d\delta^*/dy^*$ at the junction point for the bed solution. Substituting this value into Equation 17, the width of the flat-bed region B_f^* is determined.

5) With the flat-bed width now known, the stress-depth distribution over the flat-bed region is generated by solving Equation 14 at equally-spaced grid points, from the center of the channel to the junction point. Once this is done, the bed solution will have been completed.

6) The geometry and stress-depth distribution of the optimal stable channel are then obtained by putting together the bed and bank solutions. To verify these, Equation 2 is now solved from the center of the composite channel to its water margin. At the center of the channel the value for δ^* yielded by Equation 14 is assumed. Theoretically, this is already the correct value for δ^* at the channel center, and it should make the scheme converge. However, since we are applying the momentum-diffusion equation to the entire channel half-width this time, it is possible that small errors will propagate as the scheme marches from the center to the water margin. By the time the water margin is reached, the error could become significant enough to prevent the scheme from converging. In such a case, a new assumed value for δ^* at the channel center would have to be determined using the Newton-Raphson method, and the process is repeated using the same composite channel geometry, until convergence is achieved. It is expected though, that the value of δ^* at the center of the channel for which the scheme converges, will not differ appreciably from the value determined using equation 16. Once convergence occurs, the resulting stress-depth distribution is compared with the composite stress-depth distribution obtained earlier. These two should be practically identical.

It must also be recalled that at the junction point, there is a discontinuity in the curvature of the channel boundary. In order to account for this, a modified Dirac-delta function is applied over a very small interval on the bed region ending at the junction point. At the beginning of this interval, $D^* = 1$ and $dD^*/y^* = d^2D^*/y^{*2} = d^3D^*/y^{*3} = 0$. The interval over which the Dirac-delta function is applied is divided into equally spaced sub-intervals. The value of d^3D^*/y^{*3} for a grid point at the end of a sub-interval is calculated using the delta function, while the values of D^* , dD^*/y^* , and d^2D^*/y^{*2} are determined by means of numerical integration. This is done for all grid points up to the junction point. From there, the numerical solution of Equation 2 can continue along the bank region.

Once convergence is achieved, the actual stress-depth distribution over the entire channel width will have been determined. Using the stress-depth distribution, the water discharge Q is determined by integrating the logarithmic rough wall law along normals to the channel boundary and over its entire width.

7) The value of δ_{cr}^* assumed at the beginning still has to be verified. To do this, the calculated value for water discharge is compared with the given value. If the two are different, a new value for δ_{cr}^* is assumed using the Newton-Raphson method. Steps 1 to 7 are repeated until the calculated and given values of water discharge match. At this point, the correct channel geometry and stress-depth distribution will have been achieved.

8) The sediment transport rate for the flat-bed region Q_s is then determined using an appropriate bedload relation.

4.1.2. WIDE CHANNEL

Wide channels exist only at a certain value of critical stress-depth δ_{cr}^* , that depends on the channel's coefficient of friction μ . These channels have a dimensionless flat-bed width greater than 5.0. For given values of δ_{cr}^* and μ , the shape of the bank region remains the same for these channels, while the flat-bed width varies depending on the discharge to be conveyed. These are discussed in more detail in the next chapter.

Given: d_{50} and d_{90} , Q , τ_{cr}^* , δ_{cr}^* , and S .

Find: D_c , B_s^* , B_f^* , bank shape, and Q_s .

Steps 1 to 3 of the previous case still apply; the only difference is that now, δ_{cr}^* is known for a given value of μ . In step 4, a value for B_f^* will have to be assumed. B_f^* can no longer be determined using Equation 17 since it is no longer unique for given values of δ_{cr}^* and μ . Steps 5 and 6 are the same. Step 7 is similar except that it is the value of B_f^* assumed in step 4 that needs to be verified instead of δ_{cr}^* . A new value for B_f^* is assumed if the computed and given values of water discharge do not match. Steps 5 to 7 are repeated until the two discharge values are in agreement. Step 8 is the same.

4.2. SEDIMENT DISCHARGE RATE AS AN INDEPENDENT VARIABLE

While intuitively, assuming Q_s as the dependent variable may seem to be the appropriate design assumption, it is also possible to specify Q and Q_s , allowing S to be the dependent variable. When dealing with shorter time scales, which is usually the case in the design of man-made structures, the slope can be considered an independent variable. For long time scales however, Q_s is usually treated as the given and S the dependent variable. This assumption is also valid when examining the response of a stream that experiences changes in sediment input from its watershed or its upstream section due to some man-made structure or modification. In order to accommodate the transport of larger or smaller amounts of sediment, the channel can adjust its slope and width. For cases in which S is the dependent variable, the following procedure applies. This procedure is illustrated by the flowchart of Figure 4.2.

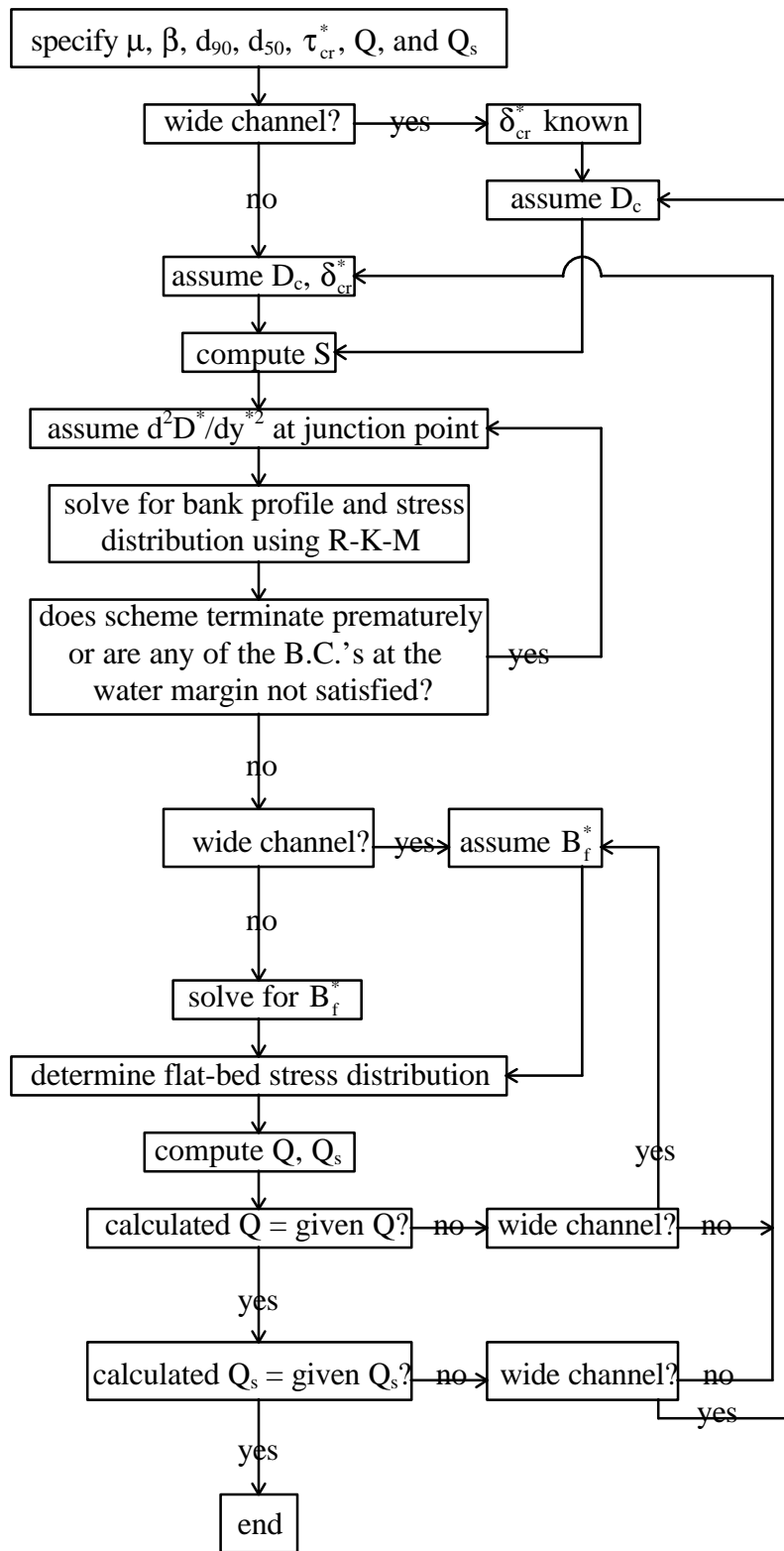


Figure 4.2. Flowchart for the case of S being the dependent variable

4.2.1. NARROW CHANNEL

Given: d_{50} and d_{90} , Q , τ_{cr}^* , and Q_s .

Find: D_c , B_s^* , B_f^* , bank shape, δ_{cr}^* and S .

- 1) Assuming δ_{cr}^* and D_c , S is calculated using Equation 20.
- 2) The bank shape, width B_s^* , and stress-depth distribution are determined by solving Equation 4.
- 3) Flat-bed width B_f^* is determined using Equation 17 and the corresponding water discharge Q is computed.
- 4) Using the value of B_f^* found in step 3 and the stress distribution, the bedload transport rate over the flat-bed region Q_s is calculated.
- 5) The computed values of Q and Q_s are compared with the given values. If either or both of the computed values do not match their corresponding given values, new values for δ_{cr}^* and D_c are assumed. Steps 1 to 5 are repeated until the calculated and given values of Q and Q_s are in agreement. At this point, δ_{cr}^* , D_c , S , B_s^* , and B_f^* are correct.

4.2.2. WIDE CHANNEL

Given: d_{50} and d_{90} , Q , τ_{cr}^* , δ_{cr}^* , and Q_s .

Find: D_c , B_s^* , B_f^* , bank shape, and S .

Steps 1 and 2 are the same as in the preceding case except that δ_{cr}^* is known. Step 3 consists of assuming a value for B_f^* and computing water discharge Q . This is compared with the given value of Q . If the two do not match, a new value for B_f^* is assumed. This step is repeated until B_f^* is such that the calculated and given values of discharge are in agreement. Step 4 is the same. In step 5, the sediment transport rate Q_s is computed and then compared with the given value. If the two do not match, a new value for D_c is assumed. Steps 1 to 5 are repeated until the calculated and given values of Q_s are in agreement.